Ultrasonics Sonochemistry 73 (2021) 105507

Contents lists available at ScienceDirect

Ultrasonics Sonochemistry

journal homepage: www.elsevier.com/locate/ultson

# Ultrasound-mediated gene delivery into suspended plant cells using polyethyleneimine-coated mesoporous silica nanoparticles

Maryam Zolghadrnasab [a], Amir Mousavi [b], Abbas Farmany [c], Ayyoob Arpanaei [a,*]

[a] Department of Industrial and Environmental Biotechnology, National Institute of Genetic Engineering and Biotechnology (NIGEB), P. O. BOX 1417863171, Tehran, Iran
[b] Department of Agricultural Biotechnology, National Institute of Genetic Engineering and Biotechnology (NIGEB), P. O. BOX 1417863171, Tehran, Iran
[c] Dental Research Center, School of Dentistry, Hamadan University of Medical Sciences, Hamadan, Iran

ARTICLE INFO

*Keywords:*
Ultrasonic treatment
Gene transfection
GUS-encoding plasmid DNA
Mesoporous silica nanoparticles

ABSTRACT

Sonoporation, ultrasound-mediated membrane perforation can potentially puncture plasma membrane and rigid cell wall on presumably reversible basis which benefit gene transfection and plant biotechnology. Herein, positively charged poly-ethyleneimine (PEI)-coated mesoporous silica nanoparticles (MSNs) with an average diameter of 100 ± 8.7 nm was synthesized for GUS-encoding plasmid delivery into the suspended tobacco cells using the ultrasound treatment. The overall potential of PEI-MSN for DNA adsorption was measured at 43.43 μg DNA $mg^{-1}$ PEI-MSNs. It was shown that high level of sonoporation may adversely upset the cell viability. Optimal conditions of ultrasonic treatment are obtained as 8 min at 3 various intensities of 160, 320 and 640 W. Histochemical staining assay was used to follow the protein expression. It was shown that PEI-coated MSNs efficiently transfer the GUS-encoding plasmid DNA into the tobacco cells. The results of this study showed that ultrasonic treatment provides an economical and straightforward approach for gene transferring into the plant cells without any need to complicated devices and concerns about safety issues.

## 1. Introduction

Plant genetic engineering has increased crop productivity in the face of the growing global population through bestowing desirable genetic traits to agricultural crops. Development of transgenic plants was an enormous modification in plant science throughout the last decades [1]. Each physical method for gene transfection, such as particle bombardment and microinjection possess inherent drawbacks, such as high cost, low efficiency, or protocol complexity; in particular, each cell is only responsive to one or a few specific methods. In recent years there are great interests to utilize an efficient and simple way for gene transfection [2]. In this respect, electroporation and ultrasound are often more versatile, as they are based on the disruption of the cell membrane and are less depend on the type of cells [3–5]. In spite of electroporation advantages, because of spatial targeting and electrode placement, electroporation has not been applied successfully in experiments with plant cells. Compared to direct DNA delivery methods, sonication (ultrasound) treatment may be simple, low cost, and no limited to the type of plant, *etc* [6,7]. However, it could cause the cell damage or rupture. To facilitate uptake, it is vital to optimize the uptake conditions without causing damage to the cells. Moderate ultrasound irradiation has been proved an efficient method for transfection *in vitro* and *in vivo* [6,8]. Ultrasound employs acoustic cavitation to create presumably reversible pores in the plasma membrane. At this time, some studies have assessed the bio-effect of ultrasound-microbubble mediated cavitation on the plant cell morphology and the cell viability is related to the peak negative pressure level [7,9–12]. Cavitation does not occur until acoustic waves reach a certain threshold intensity, at neat-threshold pressure an increasing level of inertial cavitation has taken place which is responsible for puncturing the cell surface on a non-specific basis. In contrast, at lower peak negative pressures and stable ultrasound-microbubble mediated cavitation, sonoporation does not occur in the plant cell and internalization of exogenous molecules is not evident [13,14]. In particular, optimized intensity and suitable treatment time should be applied to prohibit ultrasound damaging effects on the DNA conformation, cell membrane and subsequent cell lysis. To assess the viability of plant cells, a sensor detects the living cell colonies by means of plant esterase determination (PE) based on the fluorimetric detection of fluorescein diacetate enzymatic hydrolysis products in the cell cultures. Recently it has been argued that esterase may be used as a

* Corresponding author.
*E-mail addresses:* arpanaei@yahoo.com, aa@nigeb.ac.ir (A. Arpanaei).

https://doi.org/10.1016/j.ultsonch.2021.105507
Received 28 April 2020; Received in revised form 2 February 2021; Accepted 26 February 2021
Available online 2 March 2021

growth and viability marker of plant cells and fluoresceine diacetate (FDA) has been selected to determine the plant esterases [15–17]. FDA hydrolysis catalysed by plant esterases and produces dissociated fluorescein (intensive green fluorescence) which its absorbance at 490 nm was used for cellular viability measurement. To avoid the DNA degradation by ultrasound treatment, genome material can be loaded-on or encapsulated within a suitable carrier [18,19]. At this time, different nanoparticles such as metal oxides, polymers or carbon and silica-based nanomaterials are employed as nano-carrier [20,21]. Recently, mesoporous silica nanoparticles (MSNs) have attracted a great deal of attention due to some exclusive characteristics such as adjustable particle size, rigid structure with high pore volume and surface area [22]. In addition, modifying MSNs surface made them as appropriate carriers for biomolecules release controlling [23,24], bioimaging [25], and protein and enzyme immobilization [26]. MSNs have also been used for gene transfection and drug delivery into mammalian cells [27,28]. In recent years, several studies have been conducted on the nanoparticles-mediated gene delivery into plant cells [19,29]. However, because of the thick wall of plant cells as a big obstacle, even entering the plant cells onto small sizes nanoparticles is a challenge and a few nano-carriers are reported for gene delivery to plant suspended cells [30,31]. Indeed, for an efficient gene transfection into plants cells using nano-carriers, a mechanical method is also needed to overcome the plant cell wall barrier and facilitate the transportation of nano-carriers through the cell wall. For instance, gene gun has been applied to transfer different biomolecules into plant protoplasts using gold nanorod-coated MSNs [32,33]. Ultrasonic treatment was employed for gene delivery into plant cells using starch nanoparticles [30], CdSe quantum dots [34] or ZnS nanoparticles [18]. It has already been shown that very small nanoparticles (<50 nm) such as poly (amidoamine) dendrimer [31], calcium phosphate [35] and mesoporous silica [36] can be used for gene transfer into the plant callus, explant or root. In this study, an efficient and simple approach was developed for the plasmid DNA (pDNA) delivery into the suspended tobacco cells using PEI-coated MSNs (PEI-MSNs). The effect of ultrasonic treatment on the gene transfection efficiency onto plant cells was investigated. DNA adsorption onto PEI-MSNs and viability of suspended tobacco cells under different ultrasonic treatment conditions were also assessed. In order to obtain the gene transfection efficiency of the method, GUS protein expression was qualitatively and quantitatively followed.

## 2. Materials and methods

### 2.1. Materials

Cetyl trimethyl ammonium bromide (CTAB, 98%), sodium hydroxide, tetraethylorthosilicate (TEOS, 99%), ethanol (99.9%), hydrochloric acid (37%), *N*-(2-aminoethyl)-3-aminopropyltrimethoxy-silane (AAS, 97%), acetic acid glacial (100%), Calf thymus DNA, Tris-HCl (0.1 M, pH 8) and sodium hypochlorite were purchased from Merck (Darmstadt, Germany). *N,N*-Dimethylformamide anhydrous (DMF), Succinic anhydride, *N*-(3-dimethylaminopropyl)-n′-ethylcarbolimide hydrochloride (EDC), *N*-Hydroxysuccinimide (NHS), Fluorescein Diacetate (FDA), Triton X-100, Murashige and Skoog (MS) medium, kinetin, 6-benzylaminopurine (BAP), and 2,4-Dichlorophenoxyacetic acid (2,4-D) were purchased from Sigma-Aldrich (St. Louis, MO, USA). Polyethyleneimine (PEI, M.W. = 10 000, 99% wt) was received from Alfa Aesar. 1X PBS (Phosphate-Buffered Saline: with composition of 137 mM NaCl, 2.7 mM KCl, 10 mM $Na_2HPO_4$ and 1.8 mM $KH_2PO_4$) were purchased from Merck. DNA (Calf Thymus) was purchased from Merck. *Nicotiana tabacum* cv. Samsun seed was supplied by National Institute of Genetic Engineering and Biotechnology (NIGEB, Iran). All reagents were used as received without further purification. Milli-Q water (18.2 MΩ cm) was used throughout the experiments.

### 2.2. Preparation of MSNs

MSNs with hexagonal pore structure were synthesized by TEOS as precursor and CTAB as template surfactant in water, according to a modified method [37]. Briefly, 0.1 g of CTAB was dissolved in a mixture of 49 mL deionized water and sodium hydroxide (2 M) at 80 °C with constant stirring (agitation speed 1500 rpm). After obtaining a clear solution, 1 mL of TEOS was added in a drop wise manner, and the mixture was stirred for 2 h. Then, the solution was centrifuged (15 min, 30 °C, 28,672×*g*). In order to remove CTAB, NPs were refluxed in an alcoholic solution of hydrochloric acid with a ratio of HCl: EtOH equal to 1:10 (v/v). After 6 h, the mixture was centrifuged and the obtained product was washed with ethanol and deionized water. Hitachi S-5500, 30 kV Electron Microscopy (BF-STEM) was used to acquire images of MSNPs. For STEM analysis, samples were prepared by evaporating a dilute solution (after dispersing in ethanol and sonicating for few min) of particles onto 300 mesh carbon-coated copper grid. Particle size analyses were performed using Microstructure Measurement software. An STEM image was chosen to be as representative. Almost 50 particles were chosen and for each particle, the diameter was calculated. Then, the data were exported to SPSS software, and histogram plotting were performed.

### 2.3. Preparation of PEI-MSNs

The PEI-MSNs were prepared by a three-step method [38]. In order to modify the surface of MSNPs through the grafting procedure N-(2-aminoethyl)-3-aminopropyltrimethoxy-silane, succinic anhydride, and polyethyleneimine were used to obtain AAS-MSNPs, carboxyl-MSNPs and PEI-MSNPs, respectively. Briefly, 100 mg MSNPs (dryed at 50–70 °C) was dispersed in ethanol for 10 min, and followed by addition of EtOH: $H_2O$: Acetic Acid (46:2:1 (v/v). Then, AAS was added into the reaction mixture, and the solution was stirred for 1 h. The synthesized AAS-MSNPs were washed with ethanol and deionized water. To achieve carboxyl-MSNPs, AAS-MSNPs were washed and dispersed in DMF (20 mL). At the same time, 0.2 g of succinic anhydride was dissolved in another batch of DMF (20 mL), and the solution was stirred under a nitrogen atmosphere. After 20 min, AAS-MSNPs was dispersed to the solution of succinic anhydride in DMF, and was stirred at room temperature for 24 h under the nitrogen atmosphere. The obtained carboxyl-MSNPs were washed with DMF and deionized water. In order to functionalize the MSNPs with PEI, carboxyl-MSNPs were first dispersed in a solution of NHS (0.2 mg $mL^{-1}$) and EDC (1 mg $mL^{-1}$) in 10 mM phosphate buffered saline (PBS 1X, pH 7.4). Afterwards, 1.5 mL of the obtained suspension were shaken for 7 min and centrifuged for 3 min (5867×*g*). A solution of 10 mL of PEI in 10 mM PBS (2 mg $mL^{-1}$) was added to each aliquot and the suspension was shaken for 1 h at room temperature. Finally, the obtained PEI-MSNPs were washed with PBS and deionized water [38,39]. Brunauer Emmett Teller (BET, BJH) (BELSORP Mini II) technique was used to evaluate the morphology, surface area, and pore size of MSNPs. FTIR spectrophotometer (BRUKER, Tensor 27) with a resolution of 4 $cm^{-1}$ using pellets made from 1 mg of each samples in 100 mg KBr was applied to evaluate the chemical structure of bare MSNs, AAS-MSNs, carboxyl-MSNs and PEI-MSNs. Zeta (ζ) potential value of nanoparticles was measured to obtain the surface charge of the nanoparticles and hydrodynamic diameters of bare MSNs, AAS-MSNs, carboxyl-MSNs and PEI-MSNs was obtained using a Malvern Zetasizer Nano instrument (S90, UK) equipped with a dynamic light scattering (DLS) system after dispersing in DI water and sonicating for few min.

### 2.4. DNA adsorption onto PEI-MSNs

To study the adsorption profile of DNA onto PEI-MSNs, different concentrations of homogenized calf thymus DNA (hctDNA), non-methylated DNA (2.0 mg $mL^{-1}$), as a model DNA molecule were

prepared in Tris-HCl buffer (0.1 M, pH 8) to obtain mass ratios of hctDNA to MSNs and PEI-MSNs of 0.04:1, 0.06:1, 0.08:1, 0.1:1, 0.14:1, 0.25:1, 0.33:1, 0.5:1, 0.87:1 and 1:1, (2 mg MSNs or PEI-MSNs in 1.5 mL solution) for 90 min. The final solutions were centrifuged (10 min, 13,201×*g*) and collected for DNA analysis using spectrophotometry technique at 260 nm. Each vial supernatant was analyzed to obtain the concentration of remaining DNA. The amount of adsorbed DNA onto MSNs was calculated by subtracting the concentration of the remaining DNA from its initial concentration.

### 2.5. Tobacco suspension cells preparation

Tobacco has played a model plant role in plant biology and biotechnology [40]. Tobacco BY-2 suspension cell cultures have some advantages like easy to scale-up for manufacturing, so can multiply up to 100-fold within 7 days with a doubling time of 16–24 h under the optimized conditions [41]. Tobacco suspended cell preparation were made according to the previously reported method [42]. Briefly, tobacco seeds were sterilized with Triton X-100 (3% w/w) and Sodium hypochlorite (NaOCl) (30% w/w) for 5 min and rinsed with sterile water. Sterilized seeds were cultured on Murashige and Skoog (MS) basal solid medium (containing the stock solution (10% v/v), sucrose (0.003% w/v) and agar (0.8% w/v) in distilled water under the dim light at 4 °C for 48 h. Then, it was kept under the light for 3–7 days at 25 °C to obtain the young leaves. In the next step, leaf fragments were transferred into the MS agar containing Kinetin (0.5% w/w) and 2,4-D (1% w/w) at 25 °C under the dim light for callus induction. The brittle callus obtained from the last culture prepared in one month was isolated and 6 g of which was transferred into 30 mL MS medium containing BAP (0.5% w/w) and 2,4-D (1% w/w) (Fig. 1a). Flasks were covered with sterile parafilm and kept in a shaking incubator under the dark condition at 25 °C (Fig. 1b). After a month of consecutive subcultures, the single-cell suspensions were obtained (Fig. 1c,d).

### 2.6. Effect of ultrasound intensity and time on the cell viability

Suspended tobacco cells were treated under various ultrasonic intensities of 160, 320 and 640 W, at 5, 8 and 10 min with 40 kHz frequency using a water bath ultrasound. Bath ultrasound (BANDELIN, sonorex digital 10p) at 40 kHz frequency was applied to tobacco cells to assess the cell viability against ultrasound waves in different ultrasonic intensities and times. Intracellular esterase activity was measured by the determination of fluorescein diacetate (FDA) concentration in the cells by Cary Eclipse Fluorescence Spectrophotometer. Application of continuous wave ultrasound was conducted for a total duration of either 5, 8, or 10 min and no pulsed ultrasound was applied (no duty cycle measurement) [43]. To measure the cell viability, the method described by Steward *et al.* was applied [16]. Briefly, samples containing tobacco cells treated with ultrasound under the various conditions were diluted (3×) with PBS (0.25 M, pH 8.75). After centrifuging (10,000×*g*, 15 min), 200 μL of supernatant was isolated and added to PBS containing fluorescein diacetate (FDA) solution (0.0125% w/w) with a mass ratio of 1:14. The suspension was incubated for 15 min at 35 °C. The samples were filtered through 0.45-μm Whatman filter to remove the cell debris. The absorbance of sample was measured at 490 nm using spectrofluorometry method and the samples cell viability was estimated.

### 2.7. Characterization and purification of pDNA

pBI221 plasmid DNA (Clontech) (pDNA, 5.7 kb; Jefferson 1987), which carries a 35S::GUS:NOS-T (nopaline synthase terminator) chimeric gene encoding β glucuronidase was prepared from *E. coli* (DH5α) culture.

The pBBI221 was purified by using a QIAprep Spin Miniprep Kit according to the manufacturer's protocol. First, for bacterial growth, a culture of 1–5 mL LB medium containing Amp antibiotic was incubated for 12–16 h at 37 °C with vigorous shaking. Harvested bacterial cells were centrifuged at 6800 × g in a table-top microcentrifuge for 3 min at

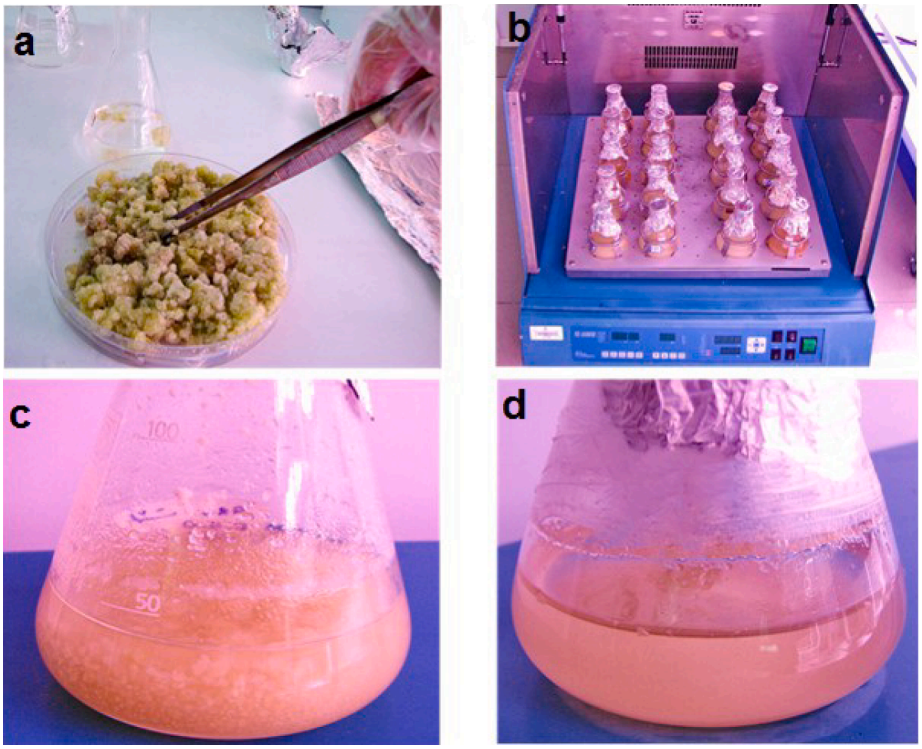


**Fig. 1.** Preparation of suspension cultures from callus. a) Picking up ~6 g callus of tobacco, transfering the callus part in 100 mL Erlenmeyer flask containing MS medium and covering the flask with sterile parafilm. b) Growing the cultures in shaking incubator under optimum conditions. c) First culture of suspended cells in a liquid medium. d) Last subculture of cell suspensions.

room temperature (RT, 15–25 °C). Then, to extract pDNA, pelleted bacterial cells were resuspend in 250 μL buffer P1 and transferred to a microcentrifuge tube. Ensured that RNase A has been added to buffer P1. Then, 250 μL buffer P2 was added and mixed gently by inverting the tube for 4–6 times. After adding 350 μL buffer N3, it was mixed immediately and thoroughly by inverting the tube for 4–6 times. The solution should become cloudy (standstill 5 min in ice). By centrifuging for 10 min at 17,900×g, a compact white pellet was formed. After discarding the precipitation, 840 μL ethanol (100%) was added to the supernatant, then gently vortex and let stand for 5 min at RT to sediment plasmid DNA. It was centrifuged for 10 min at 17,900×g to visit transparent pellet at the bottom of the microtube. Finally, the pellet was washed with 100 μL ethanol (70%), and then centrifuged for 4 min at 16,000×g. To discard the flow-through completely, the microtube was put inverted on a paper to emit the alcohol. Miniprep procedure could be analyzed using agarose gel electrophoresis [44].

### 2.8. Preparation of pDNA-PEI-MSNs conjugate

To conjugate, 10 μg $mL^{-1}$ pDNA in PBS (0.15 M, pH 7.5), was incubated with PEI-MSNs sample at a concentration of PEI-MSNs (2 mg $mL^{-1}$), then shaken for 24 h, and centrifuged at 4676 × g for 10 min in order to ensure that all nanoparticles were removed from the solution. The supernatant was collected and analyzed by using a Beckman DU 530 UV Vis spectrophotometer at 260 nm. The amount of pDNA conjugate to PEI-MSNs was calculated by subtracting the pDNA content in the supernatants from the initial concentration of pDNA. All measurements were repeated three times.

In particular, $m_{DNA\ adsorbed} = (C_{DNA\ (original)} - C_{DNA\ (supernatant)}) \times V_{system}/m_{material}$

$m_{DNA\ adsorbed}$: μg $mg^{-1}$, $C_{DNA}$: μg $mL^{-1}$, $V_{system}$: mL, $m_{material}$: mg

The adsorption of pBI221 onto PEI-MSN nanoparticles was evaluated by agarose gel (1%) electrophoresis [45,46].

### 2.9. Stability of pDNA-PEI-MSNs conjugate

To assess the stability of pDNA-PEI-MSNs conjugate, 1.5 μL of BamHI (special restriction enzyme of GUS gene on pBI221) was added separately to 3 μL of naked pDNA and the as-prepared pDNA-PEI-MSNs conjugate was incubated for 1.5 h at 37 °C. The samples were subsequently treated with 3–4 μL 10 × loading buffer to inactivate BamHI digestion. All the above solutions were run in a 1% gel stained with ethidium bromide at 100 V for 1 h.

### 2.10. Ultrasound-assisted PEI-MSNs-mediated gene delivery into plant cells

After ultrasound treatment, to obtain the higher uptake efficiency without causing cells damage, the sonication condition was optimized [6,18,30]. Among 3 different sound duration of 5, 8 and 10 min, optimum condition was considered as the average treatment time (8 min in various intensities of 160, 320 and 640 W). For plant transfection, 220 μL of pDNA-PEI-MSNs solution containing 0.1 μg pDNA was transferred into the tobacco cell suspension (1.5 mL). All samples were suspended for 24 h. Sonicated samples with different conditions are indicated in Table 1. To evaluate the GUS expression, histochemical assay [47] and GUS quantitative assessment were carried out [48]. Briefly, to perform the histochemical GUS assay, 20 μL of transfected cell suspension was transferred into a 0.5 mL Eppendorf vial containing 60 μL X-Gluc stain, then incubated for 24–48 h at 37 °C. After staining, each sample was rinsed in 70% ethanol for at least 5 min. Finally, samples were centrifuged with 4676 × g for 10 min and analyzed. To quantitatively assess the GUS, 1 mL GUS extraction buffer, including 20 mM phosphate buffer (pH 7.5), 10 mM β-mercaptoethanol and Triton X-100 (0.1%) was added to 10 mg of transfected cells. After intense vortex, samples were centrifuged with 17,900×*g* for 5 min. pNPG substrate with final concentration of 1 mM was augmented to supernatant of centrifuged samples. pNPG concentration was monitored spectrophotometrically at 405 nm after 4 and 24 h while incubating in 37 °C.

**Table 1**
Samples of cell suspension with different treatment conditions.

| Treatment condition | Sample description | Sample |
|---|---|---|
| Without Ultrasound | Cell suspension | A |
| Without Ultrasound | Cell suspension + pBI221 | B |
| Ultrasound/ 160 W – 8 min | Cell suspension + pBI221 | C |
| Ultrasound/ 320 W – 8 min | Cell suspension + pBI221 | D |
| Ultrasound/ 640 W – 8 min | Cell suspension + pBI221 | E |
| Without ultrasound | Cell suspension + pBI221-PEI-MSN | D |
| Ultrasound/ 160 W – 8 min | Cell suspension + pBI221-PEI-MSN | E |
| Ultrasound/ 320 W- 8 min | Cell suspension + pBI221-PEI-MSN | F |
| Ultrasound/ 640 W – 8 min | Cell suspension + pBI221-PEI-MSN | G |

### 2.11. Statistical analysis

All data were analyzed using the statistical package SPSS. The data were analyzed by three-way repeated measurment. The sample mean and standard error were calculated for both cell viability measurements and pDNA transfection experiment. To determine the statistical significance of the post-sonoporation level of tobacco cell viability under various intensities and treatment durations, one-way and two-way ANOVA analysis was performed to compare the measurements in the sonoporated cell groups with different treatment times against those irradiated in various intensities. Statistically significance for all cases was considered at 99% level ($p < 0.01$).

## 3. Results and discussion

### 3.1. Synthesis and characterization of PEI-MSNs

Spherical MSNs were synthesized by surfactant (CTAB) template removing method and were visualized by scanning transmission electron microscopy (STEM, Fig. 2A). The STEM images of MSNs sample show that MSNs with uniform particle size present well-ordered 2D hexagonal dot patterns. By measuring the diameters of 50 individual spheres directly from STEM image using Microstructure Measurement software, a relatively narrow size distribution of 100 ± 8.7 nm was obtained (Fig. 2B). Dynamic light scattering (DLS) reveals that MSNs and PEI-MSN had an average size of 112 ± 8 nm and 577 ± 20 nm, respectively. However, DLS measurements revealed that the size of particles increases through surface functionalization in the order of bare MSNPs < AAS-MSNPs < carboxyl MSNPs < PEI-MSNPs (Table 2). Obviously, these sizes are larger than those determined by STEM, most likely due to the absorbing of the hydrophilic polymer layers in the aqueous solution and/or aggregation of functionalized MSNPs. The hydrodynamic diameter of the bare MSNPs (112 ± 8 nm) was not much larger than that determined by STEM (100 ± 8.7 nm). However, this difference is possibly due to the mild aggregation of the bare MSNPs [49]. Silanol groups existing on the MSNs surface can be functionalized by silanization method. The surface functionalization of silica nanoparticles with cationic agents from small aminopropyl groups like amino propyl trimethoxy silane [50] to large polycations such as PEI [51] or poly-L-lysine (PLL) [18] increase the attractive electrostatic interactions between cationic MSNs surfaces and genome materials by covering the negatively charged silanol groups and introducing the positive amine groups. In this study, MSNs were coated with PEI by using a 3-step procedure. AAS was used to prepare the amine-coated MSNs. Then, carboxyl groups were introduced onto the particle surface to facilitate an efficient surface coating by PEI on the MSNs surface [52]. In the third step, branched PEI polymer molecules were covalently bonded to carboxyl-groups. To evaluate the surface charges of bare, AAS-, carboxyl- and PEI-MSNs, surface zeta (ξ) potential of nanoparticles were

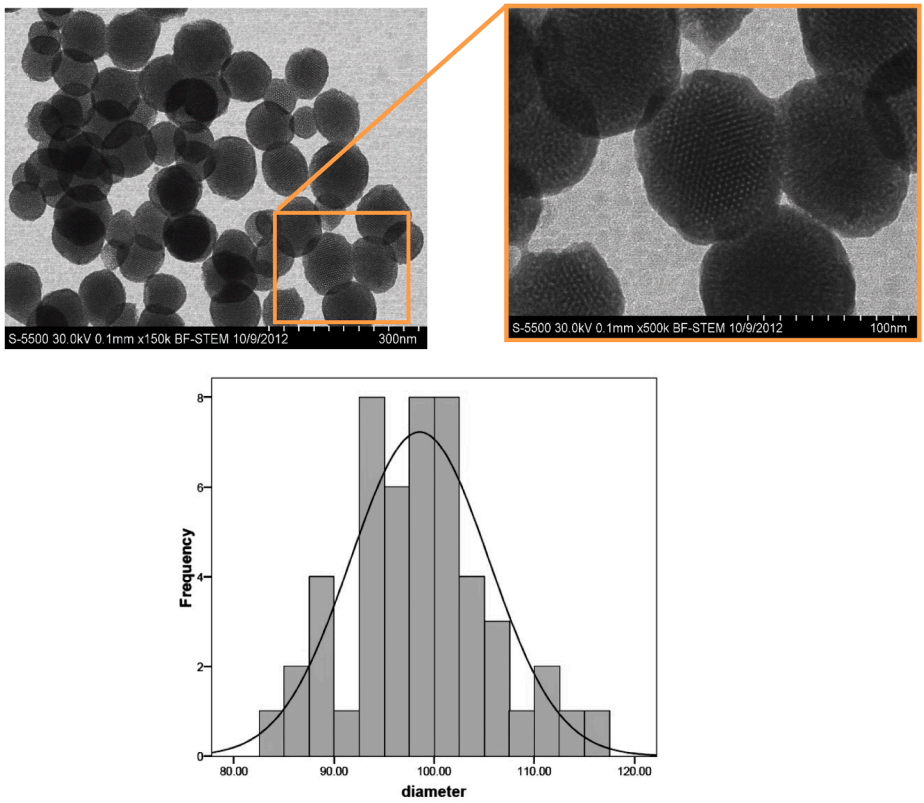


**Fig. 2.** A. Scanning transmission electron microscopy (STEM) images of MSNs. 2B Particle size distribution of MSNs.

**Table 2**
Zeta potential of MNSs, AAS-MSNs, Carboxyl-MSNs and PEI-MSNs.

| Samples | MSNs | AAS-MSNs | Carboxyl-MSNs | PEI-MSNs |
|---|---|---|---|---|
| ζ potential (mV) | −16.10 | +11.80 | −5.68 | +24.50 |
| DLS Size (nm) | 112 ± 80 | 339 ± 10 | 498 ± 14 | 577 ± 20 |

obtained. The obtained results showed that bare MSNs surface is negatively charged with ξ potential of −16.1 mV (Table 2). To modify MSNs ξ potential, their surface was functionalized with AAS. Introducing carboxyl groups on the MSNs surface decrease their surface charge to −5.68 mV. Finally, PEI-MSNs have a strong positive charge indicated by their large ξ potential of + 24.5 mV. Hyperbranched-PEI molecules existing on the as-prepared PEI-MSNs surface resulted in strong electrostatic attractions with genome materials containing negatively charged phosphate groups.

The surface and adsorption cumulative volumes of MSNs and PEI-MSNs were determined by $N_2$ adsorption desorption isotherm analysis. As shown in Fig. 3, according to the IUPAC nomenclature, $N_2$ adsorption desorption isotherm is classified as type IV isotherm with a hysteresis loop [53]. The hysteresis loop at $p/p_0$ of 0.3–0.4 can be attributed to inter-particle porosity of mesoporous silica materials [53,54]. The specific surface area of MSNs and PEI-MSNs are 964.96 and 979.27 $m^2/g$, respectively with mesoporous volumes of 1.625 and 7.745 $cm^3/g$, respectively. MSNs shows a mesoporous structure with pore size of about 6.73 nm, which are characterized by BET analysis (Fig. 3).

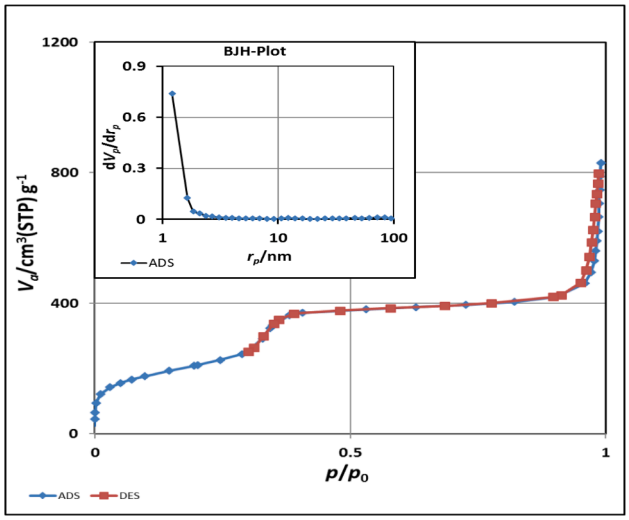


**Fig. 3.** Adsorption/desorption isotherms of MSNs and PEI-MSNs.

### 3.2. FTIR analysis

The chemical structure of bare, AAS-, carboxyl- and PEI-MSNs were analyzed with FITR spectroscopy and the results are presented in Fig. 4. Typical (Si—OH), (Si—O—Si), $H_2O$ and (O—H) groups of silica's nanoparticles are registered at 991–821, 1113, 1650 and 3478 $cm^{-1}$, respectively (Fig. 4a). As shown in Fig. 4b, amination process in the AAS-MSNs synthesis, strongly decreased the characteristic peaks for silica nanoparticle. New absorption spectra at 1650–1580, 1659, 2953–2835 and 3500–3300 $cm^{-1}$ are assigned to (—N—H bending), (—C—N stretching), (—C—H stretching) and (—N—H stretching) of AAS-MSNs, respectively. 1413, 1750–1700 and 1690–1630 $cm^{-1}$ absorption peaks are assigned to carboxyl groups (—COOH), (C═O vibration) and (amide C═O stretch) of carboxyl-MSNs, respectively (Fig. 4c). As shown in Fig. 4d, the characteristic absorption bands at 3500–3300 $cm^{-1}$ and 2953–2835 $cm^{-1}$, can be attributed to —N—H and —C—H stretching vibrations of PEI molecules, respectively [55,56].

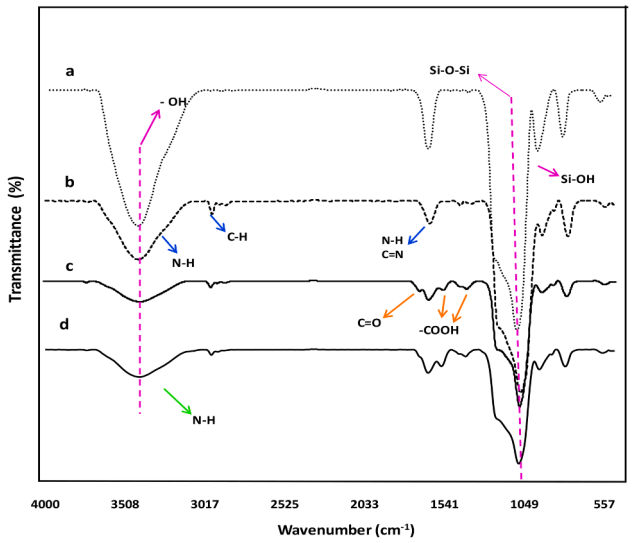


**Fig. 4.** FTIR spectra of a bare MSNs b AAS-MSNs c carboxyl-MSNs d PEI-MSNs samples.

### 3.3. Homogenized calf thymus DNA adsorption on PEI-MSNs

Homogenized calf thymus DNA (hctDNA) was used to study the DNA adsorption capacity on PEI-MSNs surface. Fig. 5 shows the adsorption isotherm of hctDNA onto PEI-MSNs at different concentrations. The obtained results show that increasing hctDNA to PEI-MSNs mass ratio from 0.04:1 to 0.14:1 leads to an increase in the hctDNA binding capacities of PEI-MSNs from 6.01 to 17.3 μg $mg^{-1}$. Furthermore, mass ratio increase to 1:1 results in increasing the adsorption capacity to 43.43 μg $mg^{-1}$.

In continue, kinetics of hctDNA adsorption onto PEI-MSNs was studied. The obtained results showed that the Langmuir model fits well with hctDNA adsorption onto PEI- MSNs with $R^2$, maximum adsorption capacity ($B_{max}$) and the reciprocal of equilibrium constant ($K_d$) of 0.99, 55.2 μg $mg^{-1}$ and 153 μg $mL^{-1}$, respectively (Fig. 5). The Langmuir model assumes a monolayer adsorption onto homogeneous surfaces [57].

It was previously reported that positively charged APTES-coated silica nanoparticles and APTES-APMS-coated silica nanoparticles have DNA adsorption capacities of 37.8 μg $mg^{-1}$ and 15.7 μg $mg^{-1}$ representively [46,58]. Lower DNA adsorption capacities of other reports instead of our study may be related to the highly positive charge enabling functionalized PEI molecules which adsorb high values of negatively charged DNA molecules. High positively chraged PEI molecules can also compress the nucleic acid molecules into small polyplex moieties which can facilitate their uptake by the cell [59]. So, higher adsorption capacity obtained in our study can be related to stronger electrostatic interactions between positively charged PEI molecules coated onto MSNs and negatively charged DNA molecules. As explained by Yetgin *et al.* [58], adsorption of calf thymus DNA molecules on the silica surfaces, changes the topology of DNA molecules from a single molecule of DNA to a super helix form.

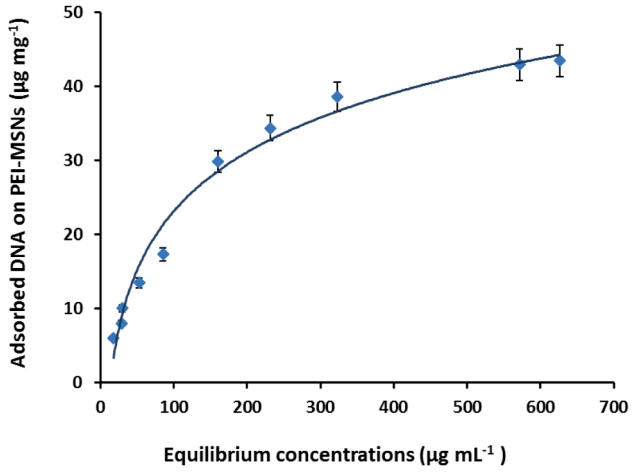


**Fig. 5.** Adsorption isotherm of hctDNA on PEI-MSNs. Adsorption tests were performed using 2 mg PEI-MSNs in 1.5 mL Tris-HCl buffer (0.1 M, pH 8) for 90 min.

### 3.4. Ultrasonic treatment effect on plant cells viability

An optimum sonication condition which causes transient permeability of the plasma membrane to facilitate the uptake without rupturing the cell, can be obtained by analyzing the sonicated cell viability measurement at different intensity and treatment times [60]. Mild ultrasound irradiation has been proved as an efficient method for transfection in animal cells and tissues *in vitro* and *in vivo* [61]. In this study, we confronted the suspended tobacco cells with ultrasound waves under 3 different times of 5, 8 and 10 min simultaneously with 3 different intensities of 160, 320 and 640 W. As shown in Fig. 6A, increases in the intensity and treatment time leads to large extents of cell rupture. Comparing the cells appearances after ultrasonic treatment, at a low ultrasonic intensity (160 W) shows that increasing the treatment

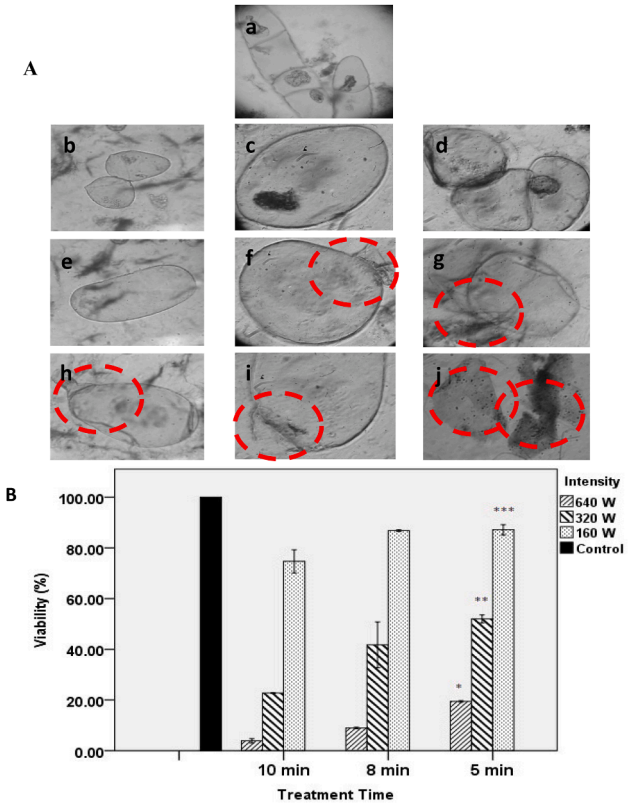


**Fig. 6.** A Light microscopy images of tobacco cells after ultrasonic treatment at various intensities and times, a Untreated cells b 160 W, 5 min. c 160 W, 8 min. d 160 W, 10 min. e 320 W, 5 min. f 320 W, 8 min. g 320 W, 10 min. h 640 W, 5 min. i 640 W, 8 min. j 640 W, 10 min. (Dashed circles indicate the damaged regions of cells). 6B The results of cellular viability assessment in tobacco cells following ultrasound treatment with different ultrasonic intensities and times. Error bars represent standard error of sample mean in plot and * Indicates statistically significant difference between different treatment intensities ($p < 0.01$).

time does not have any significant damaging effects on the cells (Fig. 6A b, c and d *vs* Fig. 6A a). However, when the ultrasonic intensity increases to 640 W with various treatment times, significant damages of cells are observed (Fig. 6A h, i and j). In contrast, lower extents of cell damages are observed when a moderate ultrasonic intensity is used (Fig. 6A e, f and g). It seems that high intensity of 640 W and long sonication time of 10 min are applied the acoustic waves reach a certain threshold intensity by which an inertial cavitation takes place. This leads to the cell membrane puncture. However, at lower sonication peak pressures obtained under the milder conditions (160 W and 5 min), the ultrasound-microbubble mediated cavitation is stabilized, and consequently sonoporation does not occur in the plant cell and internalization of exogenous molecules is not evident [10,13,14]. An accurate method was employed to determine the plant cell viability based on intracellular esterase activity in which fluorescein diacetate (FDA) is broken-up in the presence of esterase enzyme released from viable cells [16,17]. Esterase activity in the cells was estimated by spectrofluorometric technique. As shown in Fig. 6B, the cell viability slightly decreases by the ultrasonic treatment at 160 W just when the treatment time of 10 min are applied. These results indicate that at ultrasonic intensity of 320 W, the cell viability was considerably decreased in comparison with the intensity of 160 W. In addition, under this condition, by increasing the treatment time to 10 min, the cell viability has considerably declined. By applying the ultrasonic intensity of 640 W, the cell viability was decreased at all treatment times. The difference of cell viability in different treatment intensities were statistically significant ($p < 0.01$). Meanwhile, in different ultrasonic durations, cell viability differences were statistically significant ($p < 0.01$).

Ultrasonic treatment can produce acoustic cavitation that induces the cell walls transient membrane permeabilization [6,10,11]. However, ultrasound treatment with high intensities and/or in long treatment times can cause the cell death [6,18,30]. Therefore, the ultrasonic intensity and treatment time should be taken into account as crucial parameters affecting the efficiency of gene transfection of plant cells. The effect of ultrasonic treatment on living cells are generally classified as thermal and non-thermal. Heating by more than a few celsius degrees above the normal biological temperature can disturb the biological systems. At high intensities, rapid heating can cause damage in the cells, but having a minor role in increasing the cell permeability. Nonthermal effects of ultrasonic cells treatments include the cavitation that causes mechanical perturbation of the individual cell membranes. This can result in transient opening of the holes in the membrane or cause the cell lysis at high intensities [6,60]. When ultrasonic treatment at high intensities and long times is performed, transient opening of holes in the membrane may be turned to permanent holes that cause the cell lysis [11]. Therefore, the intensity and duration of ultrasonic treatment affect the suspended tobacco cells rupture and viability.

Although the cell damage occurs in fewer extents when lower ultrasonic intensities are applied, it may not be efficient enough to increase the cell membrane permeability required for an efficient transfer of material into the cell. In other words, increasing the ultrasonic intensity to 320 W or 640 W, despite the increased cell damage, is crucial to achieve the desired cell permeability for DNA-loaded nanoparticles. Liu *et al.* showed that both ultrasonic intensity and time in the ranges of 120–300 W and 3–11 min, respectively, have remarkable impacts on the cell membrane permeability and consequently, the transfer of poly-L-lysine-coated starch nanoparticles into the Dioscrea Zigiberensis G H Wright cells [30]. Applying high intensity and long exposure times of ultrasonic treatment (640 W, 10 min) will cause disruption in the cell wall; on the contrary, faint intensity level and short-time ultrasound will pierce small and a few holes through the cell wall that are insufficient for introducing nanocarriers into the cells (160 W, 5 min). Therefore, the optimized strength and time of the applied ultrasound were determined based on the cell viability assessment results. According to our results, a moderate ultrasonic time, *i.e.* 8 min, can be chosen to obtain an acceptable cell viability with low and moderate treatment intensities.

### 3.5. Preparation and stability of pDNA-PEI-MSNs conjugate

After loading pDNA onto PEI-MSNs, the obtained adsorption capacity of PEI-MSNs is obtained for pDNA as ~ 9.2 μg pDNA $mg^{-1}$ PEI-MSNs. Initial concentrations of pDNA and PEI-MSNs were 0.01 and 1 mg $mL^{-1}$, respectively. Agarose gel electrophoresis was used to confirm the pDNA adsorption onto PEI-MSNs (Fig. 7A). While free pDNA migrates-down in the gel (Lane 2, Fig. 7A), the remaining plasmid in the supernatant after loading does not have any specific band on the gel due to its very low concentration (Lane 3, ,Fig. 7A). However, the pBI221 pDNA-PEI-MSNs complex is completely trapped in the top well of agarose gel and show a very bright band (Lane 4, Fig. 7A). This lane can be used as a control of enzymatic digestion in agarose gel electrophoresis (Fig. 6B) (pDNA-PEI-MSN conjugates before enzymatic digestion). These results indicate that a significant amount of pDNA is adsorbed onto PEI-MSNs and consequently, is prevented from moving in the gel. As shown in Fig. 7 (Lane 5), unloaded PEI-MSNs does not show any bright band in the gel which was expected.

pDNA-PEI-MSNs conjugate was incubated with BamH I endonuclease to assess the stability of complexes against enzymatic degradation. As shown in Fig. 7B, free pDNA (Lane 2) was degraded completely by BamH I. The retention of pDNA is still seen around the sample well (Lane 3, Fig. 7B). However, it is noteworthy that electrophoresis shift migrated in lane 3, which suggests that the corresponding sample can partially protect pDNA from enzymatic degradation. Therefore, lane 3 may be good reagent for pDNA adsorption and protection and further for gene delivery.

pDNA before loading on MSN, has a rope-like structure with an average loop size 50 nm, some micrometers in length and 2–3 nm in width. TEM imaging by immune-gold labelling technique shows that pDNA after loading on SNPs-PEI denoting a coiled rope-like structure with a width of less than 20 nm [62].

### 3.6. pDNA transfection into tobacco suspended cells

In continue, pDNA-loaded PEI-MSNs complex was introduced into tobacco suspended cells using ultrasonic treatment intensities (160, 320 or 640 W) and 8 min treatment time. In order to quantify the gene transfection efficiency, a spectrophotometry method was applied based on the GUS enzyme specific activity assay. As shown in Fig. 8, applying PEI-MSNs is crucial to achieve a successful gene transfection to tobacco suspended cells. However, applying ultrasonic treatment for 8 min, regardless of ultrasonic treatment intensity (160, 320 or 640 W),

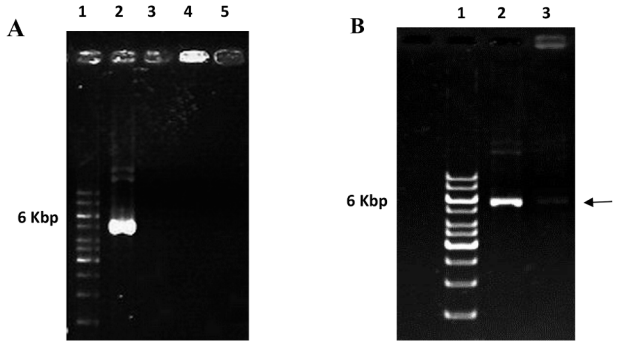


**Fig. 7.** A Gel electrophoresis test indicate the binding pBI221 plasmid onto PEI-MSNs. Lane 1, DNA marker; Lane 2, free pBI221 plasmid with 10 μg $mL^{-1}$ concentration; Lane 3, pBI221 plasmid solution with an estimated concentration of 0.8 μg $mL^{-1}$ (the supernatant resulted from plasmid adsorption samples); Lane 4, pDNA-PEI-MSNs conjugate before enzymatic digestion. Lane 5, the unloaded PEI-MSNs. 7B Agarose gel electrophoresis assay of pDNA and pDNA-PEI-MSNs conjugate; Lane 1, DNA marker; Lane 2, free pDNA (6 kbp); Lane 3, pDNA-PEI-MSNs conjugate after enzymatic digestion with faint electrophoresis shift.

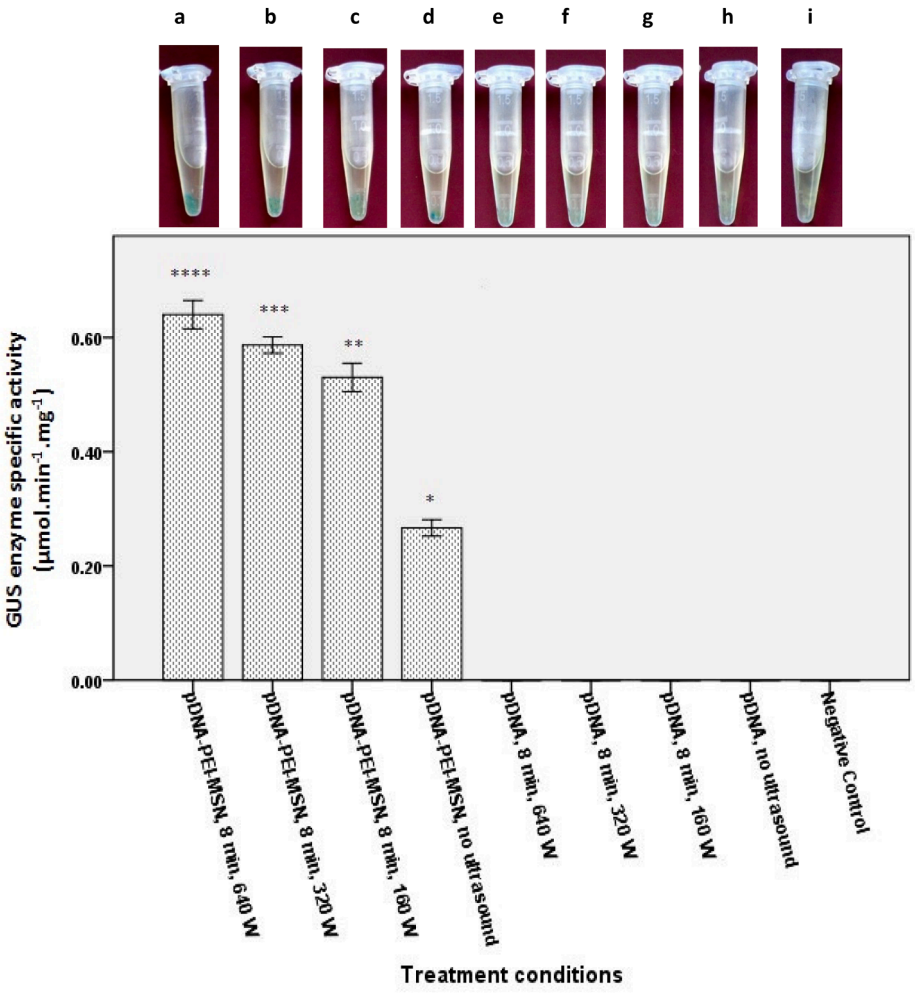


**Fig. 8.** GUS gene transfection efficiency of tobacco cells in a suspended culture in terms of GUS enzyme specific activity. GUS enzyme activity difference is significant for samples a, b, c and d.* indicates statistically significant difference between various treatment groups ($p < 0.01$).

considerably increases the gene transfection efficiency (Fig. 8). Increasing the ultrasonic intensity from 160 to 640 W resulted in a slight increase in the gene transfection efficiency (Fig. 8 a-c), possibly due to an increase in the cell permeability caused by stronger ultrasonic waves despite of cell rupturing in some cases (Fig. 6A,i). Histochemical GUS assay of tobacco cell suspensions showed that when the free plasmid molecules is introduced into the cells, in the absence of ultrasonic treatment and MSNs, no color change can be observed in the collected cells. These results indicate an unsuccessful gene transfection process due to the presence of an impermeable plant cell wall against free pDNA molecules (Fig. 8h). Same results are obtained in the presence of ultrasonic treatment of free pDNA even with sonication exposure of different intensities at 8 min (Fig. 8e-g), possibly due to degradation of pDNA by the applied ultrasonic waves. However, pDNA-PEI-MSNs without any ultrasonic treatment led to appearance of blue color in the collected cells which show an efficient gene transfection to tobacco cells (Fig. 8d). This result implies that PEI-MSNs have the ability to pass through the plant wall cells, possibly due to their strong positively charged surfaces and consequently their attractive electrostatic interactions with plant cell surface with a negative charge [63], leading to cellular uptake of nanoparticles and then, their facilitated internalization into the cells. Interestingly, very efficient gene transfection to tobacco cells was obtained for pDNA-loaded PEI-MSNs and ultrasonic treatment was applied and indicated by obvious color changes of treated samples while their GUS enzyme activity are different (Fig. 8a-c). Statistical analysis reveals that there is a significant differences between pDNA-PEI-MSN groups with different intensities and without ultrasound application (Fig. 8a-d, $p < 0.01$). This result implies that PEI-MSNs can protect the pDNA degradation against ultrasonic waves, while later increases the plant cell wall permeability and facilitate pDNA-loaded PEI-MSNs passing through the cell wall. The synergistic effect of these two parameters considerably increases the gene transfection efficiency.

Yu-Qin *et al.* [18] shown that poly-*L*-lysine-coated ZnS nanoparticles with an average size of 3–5 nm efficiently deliver GUS-encoding plasmid into young tobacco leaves using the ultrasonic treatment. Efficiency of gene transfection of the treated tobacco plant under various conditions indicated that highest efficiency is achieved when an ultrasonic treatment with intensity of 60 W for 20 min is applied. These results indicate that the optimum condition for the ultrasonic treatment to achieve highest gene transfection efficiency depends on the plant type (protoplast, cells, leaves, roots, *etc.*) as well as nanocarriers and their size.

## 4. Conclusion

In conclusion, an efficient method was developed for the gene transfection in plant suspended cells using pDNA-loaded PEI-MSNs and ultrasonic treatment. The obtained results reveales that high amount DNA can be adsorbed onto PEI-MSNs. Investigating the effect of ultrasonic treatment on the tobacco plant cell viability showed that increasing the ultrasonic intensity from 160 to 320 W and further increase to 640 W lead to striking damages of plant cells while increasing the treatment time has milder degradation effects. Study of the gene

transfection efficiency of plant cells under different conditions showed that applying the PEI-MSNs as gene carrier is crucial to obtain any efficient gene delivery into plant cells; however, utilizing ultrasonic treatment has a synergistic effect on the gene delivery and can considerably enhance the gene transfection efficiency. Indeed, pDNA molecules are effectively protected from degradation caused by ultrasonic treatment once loaded onto the positively charged PEI-MSNs, while free pDNA molecules are probably damaged under the same conditions leading to an unsuccessful gene transfection. Applying high ultrasonic intensities resulted in lower gene transfection efficiency due to decrease in the cell viability through damaging the cell wall. The obtained results indicate that combination of PEI-MSNs and ultrasonic treatment provides an efficient and simple approach for gene transfection of the plant cells. In general, applying ultrasonic treatment associated with PEI-MSNs nanocarrier is an efficient approach in gene delivery into suspended plant cells.

## CRediT authorship contribution statement

**Maryam Zolghadrnasab:** Data curation, Writing - original draft, Visualization, Investigation, Writing - review & editing. **Amir Mousavi:** Conceptualization, Methodology, Software, Data curation, Writing - original draft, Visualization, Investigation, Supervision, Software, Validation, Writing - review & editing. **Abbas Farmany:** Software, Validation, Writing - review & editing. **Ayyoob Arpanaei:** Conceptualization, Methodology, Software, Data curation, Writing - original draft, Visualization, Investigation, Supervision, Software, Validation, Writing - review & editing.

## Declaration of Competing Interest

The authors declare that they have no known competing financial interests or personal relationships that could have appeared to influence the work reported in this paper.

## Acknowledgements

The authors would like to thank National Institute of Genetic Engineering and Biotechnology (NIGEB) for providing instrumentation facilities.

## References

[1] B.D. Prasad, T. Ranjan, S. Sahni, V. Sharma, The recent advances in transgenic crops: a review, J. Cell Tissue Res. 17 (2017) 6185–6196.
[2] E. Kościańska, K. Wypijewski, Electroporated intact BY-2 tobacco culture cells as a model of transient expression study, Acta Biochim. Pol. 48 (3) (2001) 657–661.
[3] H. Potter, R. Heller, Transfection by electroporation, Curr. Protoc. Mol. Biol. CHAPTER (2003) Unit-9.3.
[4] P. Vankan, W. Filipowicz, Structure of U2 snRNA genes of Arabidopsis thaliana and their expression in electroporated plant protoplasts, EMBO J. 7 (3) (1988) 791–799.
[5] G.L. Prasanna, T. Panda, Electroporation: basic principles, practical considerations and applications in molecular biology, Bioprocess Eng. 16 (1997) 261–264.
[6] Y. Liu, H. Yang, A. Sakanishi, Ultrasound: mechanical gene transfer into plant cells by sonoporation, Biotechnol. Adv. 24 (2006) 1–16.
[7] C.-W. Lo, C. Desjouy, S.-R. Chen, J.-L. Lee, C. Inserra, J.-C. Béra, W.-S. Chen, Stabilizing in vitro ultrasound-mediated gene transfection by regulating cavitation, Ultrason. Sonochem. 21 (2) (2014) 833–839.
[8] M.L. Choudhary, C.K. Chin, Ultrasound mediated delivery of compounds into petunia protoplasts and cells, J. Plant Biochem. Biotechnol. 4 (1) (1995) 37–39.
[9] J.A. Wyber, J. Andrews, A. D'emanuele, The use of sonication for the efficient delivery of plasmid DNA into cells, Pharm. Res. 14 (1997) 750–756.
[10] P. Qin, L. Xu, W. Zhong, A.C.H. Yu, Ultrasound-microbubble mediated cavitation of plant cells: effects on morphology and viability, Ultrasound Med. Biol. 38 (6) (2012) 1085–1096.
[11] A.C.H.Y. Peng Qin, X. Lin, P. Cai, Hu Yaxin, Subcellular impact of sonoporation on plant cells: Issues to be addressed in ultrasound-mediated gene transfer, Ultrason. Sonochem. 20 (2013) 247–253.
[12] S. Chang, J. Guo, J. Sun, S. Zhu, Y. Yan, Y. Zhu, M. Li, Z. Wang, R.X. Xu, Targeted microbubbles for ultrasound mediated gene transfection and apoptosis induction in ovarian cancer cells, Ultrason. Sonochem. 20 (1) (2013) 171–179.
[13] M. Ashokkumar, The characterization of acoustic cavitation bubbles – an overview, Ultrason. Sonochem. 18 (4) (2011) 864–872.
[14] W.-S. Chen, A.A. Brayman, T.J. Matula, L.A. Crum, Inertial cavitation dose and hemolysis produced in vitro with or without Optison®, Ultrasound Med. Biol. 29 (5) (2003) 725–737.
[15] J. Vitecek, J. Petrlova, V. Adam, L. Havel, K. Kramer, P. Babula, R. Kizek, A fluorimetric sensor for detection of one living cell, Sensors 7 (3) (2007) 222–238.
[16] N. Steward, R. Martin, J.M. Engasser, J.L. Goergen, A new methodology for plant cell viability assessment using intracellular esterase activity, Plant Cell Rep. 19 (2) (1999) 171–176.
[17] S. Johnson, V. Nguyen, D. Coder, Assessment of cell viability, Curr. Protoc. Cytom. SUPPL.64 (2013) 9.2.1-9.2.26.
[18] F. Yu Qin, L. Lu Hua, W. Pi Wu, Q. Jing, F. Yong Ping, W. Hui, S.L. Jing Ran, Chang Li, Delivering DNA into plant cell by gene carriers of ZnS nanoparticles, Chem. Res. Chinese Univ. 28 (2012) 672–676.
[19] I. Sanzari, A. Leone, A. Ambrosone, Nanotechnology in plant science: to make a long story short, Bioeng. Biotechnol. 7 (2019) 1–12.
[20] S.A. Kuznetsova, T.S. Oretskaya, Nanoparticulate delivery systems for targeted delivery of nucleic acids to cells, Nanotechnologies Russ. 5 (9-10) (2010) 583–600.
[21] Z. Li, X. Du, X. Cui, Z. Wang, Ultrasonic-assisted fabrication and release kinetics of two model redox-responsive magnetic microcapsules for hydrophobic drug delivery, Ultrason. Sonochem. 57 (2019) 223–232.
[22] Z. Li, J.C. Barnes, A. Bosoy, J.F. Stoddart, J.I. Zink, Mesoporous silica nanoparticles in biomedical applications, Chem. Soc. Rev. 41 (7) (2012) 2590.
[23] J.Y. Choi, B. Gupta, T. Ramasamy, J.-H. Jeong, S.G. Jin, H.-G. Choi, C.S. Yong, J. O. Kim, PEGylated polyaminoacid-capped mesoporous silica nanoparticles for mitochondria-targeted delivery of celastrol in solid tumors, Colloids Surf. B Biointerfaces. 165 (2018) 56–66.
[24] G. Pan, T.-ting. Jia, Q.-xia. Huang, Y.-yan. Qiu, J. Xu, P.-hao. Yin, T. Liu, Mesoporous silica nanoparticles (MSNs)-based organic/inorganic hybrid nanocarriers loading 5-Fluorouracil for the treatment of colon cancer with improved anticancer efficacy, Colloids Surf. B. Biointerfaces 159 (2017) 375–385.
[25] C.-W. Lu, Y. Hung, J.-K. Hsiao, M. Yao, T.-H. Chung, Y.-S. Lin, S.-H. Wu, S.-C. Hsu, H.-M. Liu, C.-Y. Mou, C.-S. Yang, D.-M. Huang, Y.-C. Chen, Bifunctional magnetic silica nanoparticles for highly efficient human stem cell labeling, Nano Lett. 7 (1) (2007) 149–154.
[26] Y. Hao, X. Yang, Y. Shi, S. Song, J. Xing, J. Marowitch, J. Chen, J. Chen, Magnetic gold nanoparticles as a vehicle for fluorescein isothiocyanate and DNA delivery into plant cells, Botany 91 (7) (2013) 457–466.
[27] Y. Zhou, G. Quan, Q. Wu, X. Zhang, B. Niu, B. Wu, Y. Huang, X. Pan, C. Wu, Mesoporous silica nanoparticles for drug and gene delivery, Acta Pharm. Sin. B 8 (2) (2018) 165–177.
[28] A. Watermann, J. Brieger, Mesoporous silica nanoparticles as drug delivery vehicles in cancer, Nanomaterials 7 (2017) 1–17.
[29] T.B.U. enhancement of gene transfection in murine melanoma tumors. U.M.B. 1999;25(9):1425–30. 1. Miller DL, Bao S, Gies RA, Nanoparticle-Mediated Delivery towards Advancing Plant Genetic Engineering, Trends Biotechnol. 1636 (2018) 1–16.
[30] J. Liu, F.-H. Wang, L.-L. Wang, S.-Y. Xiao, C.-Y. Tong, D.-Y. Tang, X.-M. Liu, Preparation of fluorescence starch-nanoparticle and its application as plant transgenic vehicle, J. Cent. South Univ. Technol. 15 (6) (2008) 768–773.
[31] K. Pasupathy, S. Lin, Q. Hu, H. Luo, P.C. Ke, Direct plant gene delivery with a poly (amidoamine) dendrimer, Biotechnol. J. 3 (8) (2008) 1078–1082.
[32] F. Torney, B.G. Trewyn, V.-Y. Lin, K. Wang, Mesoporous silica nanoparticles deliver DNA and chemicals into plants, Nat. Nanotechnol. 2 (5) (2007) 295–300.
[33] S. Martin-Ortigosa, J.S. Valenstein, V.-Y. Lin, B.G. Trewyn, K. Wang, Gold functionalized mesoporous silica nanoparticle mediated protein and DNA codelivery to plant cells via the biolistic method, Adv. Funct. Mater. 22 (17) (2012) 3576–3582.
[34] Q. Wang, J. Chen, H. Zhang, M. Lu, D. Qiu, Y. Wen, Q. Kong, Synthesis of water soluble quantum dots for monitoring carrier-DNA nanoparticles in plant cells, J. Nanosci. Nanotechnol. 11 (3) (2011) 2208–2214.
[35] S. Naqvi, A.N. Maitra, M.Z. Abdin, M. Akmal, I. Arora, M. Samim, Calcium phosphate nanoparticle mediated genetic transformation in plants, J. Mater. Chem. 22 (8) (2012) 3500.
[36] F.-P. Chang, L.-Y. Kuang, C.-A. Huang, W.-N. Jane, Y. Hung, Y.-ie C. Hsing, C.-Y. Mou, A simple plant gene delivery system using mesoporous silica nanoparticles as carriers, J. Mater. Chem. B. 1 (39) (2013) 5279.
[37] F. Hoffmann, M. Cornelius, Jürgen Morell, M. Fröba, Silica-based mesoporous organic–inorganic hybrid materials, Angew. Chem. Int. Ed. 45 (20) (2006) 3216–3251.
[38] N. Taebnia, D. Morshedi, M. Doostkam, S. Yaghmaei, F. Aliakbari, G. Singh, A. Arpanaei, The effect of mesoporous silica nanoparticle surface chemistry and concentration on the α-synuclein fibrillation, RSC Adv. 5 (75) (2015) 60966–60974.
[39] J.M. Rosenholm, A. Penninkangas, M. Lindén, Amino-functionalization of large-pore mesoscopically ordered silica by a one-step hyperbranching polymerization of a surface-grown polyethyleneimine, Chem. Commun. (37) (2006) 3909–3911.
[40] T. Nagata, Y. Nemoto, S. Hasezawa, Tobacco BY-2 cell line as the "HeLa" cell in the cell biology of higher plants, Int. Rev. Cytol. 132 (1992) 1–30.
[41] R.B. Santos, R. Abranches, R. Fischer, M. Sack, T. Holland, Putting the spotlight back on plant suspension cultures, Front. Plant Sci. 7 (2016) 1–12.
[42] A. Iantcheva, M. Vlahova, A. Atanassov, A.S. Duque, S. Araújo, D.F. Dos Santos, P. Fevereiro, Cell suspension cultures, Medicago truncatula handbook, Ardmore, 2006.

[43] O. Sarheed, Development of an optimised application protocol for sonophoretic transdermal delivery of a model hydrophilic drug, Open Biomed. Eng. J. 5 (1) (2011) 14–24.
[44] QIAprep® Miniprep Handbook, n.d. www.qiagen.com.
[45] D.R. Radu, C.-Y. Lai, K. Jeftinija, E.W. Rowe, S. Jeftinija, V.-Y. Lin, A polyamidoamine dendrimer-capped mesoporous silica nanosphere-based gene transfection reagent, J. Am. Chem. Soc. 126 (41) (2004) 13216–13217.
[46] H. Yang, K. Zheng, Z. Zhang, W. Shi, S. Jing, L. Wang, W. Zheng, D. Zhao, J. Xu, P. Zhang, Adsorption and protection of plasmid DNA on mesoporous silica nanoparticles modified with various amounts of organosilane, J. Colloid Interface Sci. 369 (1) (2012) 317–322.
[47] R.A. Jefferson, T.A. Kavanagh, M.W. Bevan, GUS fusions: beta-glucuronidase as a sensitive and versatile gene fusion marker in higher plants, EMBO J. 6 (1987) 3901–3907.
[48] A. Falciatore, F. Formiggini, C. Bowler, Reporter genes and in vivo imaging, in: P. M. Gilmartin, C. Bowler (Eds.), Mol. Plant Biol. a Pract. Approach, Oxford University Press, 2002, pp. 265–284.
[49] E. Hashemi, H. Mahdavi, J. Khezri, F. Razi, M. Shamsara, A. Farmany, Enhanced gene delivery in bacterial and mammalian cells using PEGylated calcium doped magnetic nanograin, Int. J. Nanomed. 14 (2019) 9879–9891.
[50] F. Gao, P. Botella, A. Corma, J. Blesa, L. Dong, Monodispersed mesoporous silica nanoparticles with very large pores for enhanced adsorption and release of DNA, J. Phys. Chem. B. 113 (6) (2009) 1796–1804.
[51] B. Ufer, J.M. Rosenholm, A. Duchanoy, L. Bergman, M. Lindén, Poly (ethylene imine) functionalized mesoporous silica nanoparticle for biological applications, Stud. Surf. Sci. Catal. 174 (2008) 353–356.
[52] N. Prabhakar, J. Zhang, D. Desai, E. Casals, T. Gulin-Sarfraz, T. Näreoja, J. Westermarck, J.M. Rosenholm, stimuli-responsive hybrid nanocarriers developed by controllable integration of hyperbranched PeI with mesoporous silica nanoparticles for sustained intracellular sirNa delivery, Int. J. Nanomed. 11 (2016) 6591–6608.
[53] V. Cauda, A. Schlossbauer, T. Bein, Bio-degradation study of colloidal mesoporous silica nanoparticles: Effect of surface functionalization with organo-silanes and poly(ethylene glycol), Microporous Mesoporous Mater. 132 (1-2) (2010) 60–71.
[54] K.S.W. Sing, Reporting physisorption data for gas/solid systems with special reference to the determination of surface area and porosity (Provisional), Pure Appl. Chem. 54 (1982) 2201–2218.
[55] K. Panwar, M. Jassal, A.K. Agrawal, In situ synthesis of Ag-SiO2Janus particles with epoxy functionality for textile applications, Particuology. 19 (2015) 107–112.
[56] X. Mei, D. Chen, N. Li, Q. Xu, J. Ge, H. Li, B. Yang, Y. Xu, J. Lu, Facile preparation of coating fluorescent hollow mesoporous silica nanoparticles with pH-sensitive amphiphilic diblock copolymer for controlled drug release and cell imaging, Soft Matter 8 (19) (2012) 5309.
[57] I. Langmuir, The adsorption of gases on plane surfaces of glass, mica and platinum, J. Am. Chem. Soc. 40 (9) (1918) 1361–1403.
[58] S.M. Solberg, C.C. Landry, Adsorption of DNA into mesoporous silica, J. Phys. Chem. B. 110 (31) (2006) 15261–15268.
[59] T. Xia, M. Kovochich, M. Liong, H. Meng, S. Kabehie, S. George, J.I. Zink, A.E. Nel, Polyethyleneimine coating enhances the cellular uptake of mesoporous silica nanoparticles and allows safe delivery of siRNA and DNA constructs, ACS Nano 3 (10) (2009) 3273–3286.
[60] M. Joersbo, J. Brunstedt, Sonication: a new method for gene transfer to plants, Physiol. Plant. 85 (1992) 230–235.
[61] P.E. Huber, P. Pfisterer, In vitro and in vivo transfection of plasmid DNA in the Dunning prostate tumor R3327-AT1 is enhanced by focused ultrasound, Gene Ther. 7 (17) (2000) 1516–1525.
[62] H. Song, M. Yu, Y. Lu, Z. Gu, Y. Yang, M. Zhang, J. Fu, C. Yu, Plasmid DNA delivery: nanotopography matters, J. Am. Chem. Soc. 139 (50) (2017) 18247–18254.
[63] S. Alila, S. Boufi, M.N. Belgacem, D. Beneventi, Adsorption of a cationic surfactant onto cellulosic fibers I. Surface charge effects, Langmuir 21 (18) (2005) 8106–8113.